

Quantum calculations for line shapes in Raman spectra of molecular nitrogen

Sheldon Green

NASA Goddard Space Flight Center, Institute for Space Studies, New York, New York 10025

Winifred M. Huo

NASA Ames Research Center, Moffett Field, CA 94035-1000

(November 7, 1995)

Abstract

Using previously described close coupling (CC) and coupled states (CS) cross sections for N_2 - N_2 collisions [*J. Chem. Phys.* **xxx**, nnn (1996)] we have calculated CARS linewidths at room temperature and below. Agreement with experimental values at room temperature is quite good but predictions become increasingly too large at lower temperatures, with errors reaching 10–30% at 113 K. We believe these low temperature discrepancies reflect errors in the intermolecular potential used here. To obtain linewidths at higher temperatures we have used the energy corrected sudden (ECS) approximation, taking the fundamental cross sections, $\sigma(0,0 \rightarrow J_1, J_2)$, from the CC-CS calculations extended to higher collision energies with additional CS and infinite order sudden (IOS) calculations; the ECS scaling distance, l_c was chosen by fitting to the 300 K CC-CS results. In general, we find rather good agreement with experimental values to 1500 K, although it appears that smaller values of l_c are more appropriate for higher temperatures and for higher rotational levels. This variability of l_c is reasonable from physical arguments but some-

what diminishes the predictive utility of this approach. Agreement of these purely ab initio predictions with experimental data is nearly as good as that obtained from the best rate law model whose parameters were fitted to these data.

I. INTRODUCTION

A great deal of experimental and theoretical effort has been expended trying to understand line shapes in Raman spectra of N_2 . [1–23] Much of this effort is driven by the need for these parameters in nonlinear Raman (CARS and SRS) thermometry, a noninvasive technique for probing temperature in environments where conventional transducers cannot readily be employed. In particular, CARS thermometry has become the method of choice for measuring temperatures in flames, explosive shocks, and engines; [24] many references to such applications were given recently by Martinsson, et al. [20] and by Dreier, et al. [22] Similar techniques have also proved useful for wind tunnel diagnostics, providing simultaneous determination of temperature, pressure, and flow velocity. [25] These applications generally require computer modeling of complex spectral line shapes in order to extract the relevant parameters and this in turn requires detailed knowledge of pressure induced linewidths, line shifts, and line coupling parameters as a function of temperature. [24]

At low pressures, where the rotational structure in the spectrum is well resolved, measurement of linewidth and line shift parameters is straightforward; in this regime line shapes are simply a sum of nonoverlapping Lorentzian profiles (Voigt profiles at very low pressures where Doppler broadening is significant). At higher pressures the lines overlap and collisions can transfer intensity among them, generally increasing intensity near the center of the band and removing intensity from the wings, leading to an apparent “collisional narrowing” of the vibrational band. The N_2 vibrational Q-branch Raman lines which are generally used in CARS thermometry are closely spaced and line coupling is important even at atmospheric pressure. In general, individual line coupling parameters cannot be measured directly (see,

however, recent work on CO [26] and on D₂ [27]). Rather, as discussed in more detail below, line coupling parameters are related to state-to-state collisional excitation rates and these rates are extracted from the data by fitting to parameterized rate law models. However, unless the models are based on accurate physics the parameters determined this way must be considered as empirical fitting parameters with little physical meaning and may provide poor estimates when extrapolated to conditions outside the range of data from which they were obtained. For example, the temperature dependence of the parameters is often found to be inadequate when extrapolated beyond the range of the input data. [20,23] Even more problematic is the use of state-to-state collision rates which were obtained by fitting to line shape models for predicting completely different phenomena such as aerothermodynamic properties used for flow field modeling. [28] At still higher pressures the vibrational band collapses to a single Lorentzian line which narrows (collisional narrowing) with increasing pressure. This regime is still described by the same line coupling theory, but, because of the strong coupling, the width of the band can be accurately represented by an effective (average) rotational relaxation rate which can be calculated from the detailed state-to-state rates. [16,21,22] At even higher pressures broadening of this single line owing to vibrational dephasing and vibrational excitation rates overcomes the collisional narrowing, but this does not occur for N₂ below about 500 atmospheres in the gas phase and, although of some interest in condensed phases, [18,19] is not considered here.

In principle the line shape parameters could be obtained by directly measuring the state-to-state rotational excitation rates, but only one such study has been reported. Sitz and Farrow [29] pumped ground vibrational state N₂ molecules to specific rotational levels in the first excited vibrational state and measured the rate of population transfer to other rotational levels in the same vibrational state. The room temperature rates obtained this way were, in fact, able to predict line shape parameters, although they differed in detail from rates extracted by fitting parameters in rate law models. Other, related data include an average rotational relaxation rate which was recently measured by probing rotational populations in an expanding supersonic molecular beam, [30] and measurement of the decay

of alignment in molecular nitrogen collisions which was recently reported by Sitz and Farrow. [31]

Several attempts have been made to predict the state-to-state rates and/or line shape parameters from first principles. This requires knowledge of the intermolecular forces as a function of collision geometry and calculation of the resulting collision dynamics. Koszykowski, et al. [8] employed an atom-atom pairwise additive Lennard-Jones potential and determined the rate constants using quasiclassical trajectory calculations. While the goal of that work was to determine Raman linewidths, they also deduced a scaling law for the rotational excitation rate constants. Using a somewhat improved interaction potential, Agg and Clary [32] reported rotational excitation rate constants calculated with the quantum mechanical infinite order sudden (IOS) approximation and also with a modified breathing sphere approximation; results were compared with linewidths over a wide temperature range. Billing and Wang [33] used a semiclassical scattering formalism along with a simple pairwise additive exponential repulsive interaction to calculate high temperature rotational relaxation and transport coefficients. Calculations for line shifts [12] and linewidths [20] using a semiclassical (Robert-Bonamy) line shape theory have also been performed; these employed pairwise atom-atom Lennard-Jones interactions plus the long-range quadrupole-quadrupole interaction, but also used a separate isotropic Lennard-Jones molecule-molecule interaction to calculate the classical trajectories. These calculations obtained the line shape parameters directly without providing detailed state-to-state collision rates. The line shifts were in reasonable accord with measurements; the linewidths were not directly compared with experimental values, but gave as good results as did parameterized rate law models for determining temperatures from rotational CARS spectra.

The most accurate $\text{N}_2\text{-N}_2$ rigid-rotor potential reported so far is that of van der Avoird, et al. [34] (vdA) which is based on ab initio calculations and adjusted to fit second virial coefficients over a wide temperature range; it also reproduces a variety of solid state properties reasonably well, although these comparisons suggested that the short-range repulsion might be somewhat too strong. Using the vdA potential, Green [35] determined rigid rotor

collision rates using the IOS approximation and the energy corrected sudden (ECS) approximation, obtaining reasonable agreement with experiment. Also using the vdA potential, Heck and Dickinson [36] used classical trajectory scattering calculations to obtain transport and relaxation cross sections, finding good agreement with the former but an inconsistent pattern for the latter which they interpreted as suggesting that the interaction may be insufficiently anisotropic in regions sampled at low energy. In a previous paper [37] we used the vdA potential along with extensive, accurate close coupling (CC) and coupled states (CS) calculations for room temperature rotational excitation and investigated the accuracy of the IOS approximation and the ECS scaling method for predicting detailed state-to-state rates. In the present work we examine predictions of these calculations for spectral line shape parameters in N_2 as a function of temperature.

The microscopic theory of line shapes is nontrivial although many aspects now appear to be well understood; in favorable cases, where accurate intermolecular potentials and collision dynamics have been used, agreement with experiment is quite satisfying. [38] However, the present system involves self-broadening and the effect of identical molecule exchange symmetry on line shapes is not fully understood currently. The Fano [39] formalism which underlies most current computational schemes starts by separating the roles of the spectroscopic molecule and the bath molecules, and suggestions in the literature for incorporating identical molecule symmetry into this paradigm do not appear to be consistent. [40–44] In any case, actual calculations based on these methods have not yet been done. As noted in our previous paper, [37] this system is amenable to a classical description in the sense that quantum interference terms between direct and exchange contributions nearly cancel for state-to-state cross sections, even though the exchange contribution itself needs to be included in the treatment. Pasmenter and Ben-Reuven [42] also argued that the effects of identical molecule symmetry on line shapes are expected to be small for vibrational spectra because the exchange terms are small in the vibrational excitation cross sections which enter into the expression of lineshapes. While the relative unimportance of the exchange term in the vibrational excitation cross section was also noted in our earlier work, [37] the contri-

bution from the change of the initial state population due to rotationally inelastic collisions includes non-negligible exchange contributions. Although we believe it is important to consider this point, perhaps using the recent formalism of Monchick [44] which appears to be quite thorough and which, unlike the Fano formalism, is based on a quantum Boltzmann equation in which identical molecule symmetry is introduced in a more natural manner, we will not consider exchange in the present work but rather treat the molecules as distinguishable particles. This will facilitate comparison with earlier studies of line shapes in N_2 all of which assumed distinguishable molecules.

A number of additional approximations are routinely used in analyzing CARS data in order to express linewidths in terms of rotational excitation rates. These were discussed in some detail by Green [35] and will be reviewed only briefly here. The major assumption is that the intermolecular forces and hence the collision dynamics depend only very weakly on the N_2 vibrational state; this is the key assumption which, for isotropic Raman spectra, leads to identification of line coupling parameters with state-to-state collision rates and which also leads to the sum rule that allows the linewidths to be calculated as the sum of collision rates out of the spectroscopic level. The contribution to the linewidths in N_2 from vibrational dephasing has been estimated from high pressure measurements to be quite small, on the order of $2.8 \pm 1.6 \times 10^{-5} \text{ cm}^{-1}\text{amagat}^{-1}$. [19] This can be compared to linewidth parameters which are on the order of $5 - 10 \times 10^{-2} \text{ cm}^{-1}\text{amagat}^{-1}$. Another necessary condition for the validity of this approximation is vanishing line shifts. In fact, the line shift parameters are found to be small, about $-0.35 \times 10^{-2} \text{ cm}^{-1}\text{atm}^{-1}$, with little temperature dependence between 300 and 1000 K, [9,12,14] although this may comprise as much as 10% of the linewidth parameter for higher temperatures and higher rotational lines. Additional support for the adequacy of this approximation comes from the finding that pure rotational Raman linewidths for the S(J) lines ($J \rightarrow J + 2$) are nearly equal to the average of those for the Q(J) and Q(J+2) lines in the vibrational Raman band. [1,20,23] The line coupling parameters (and by the sum rule the linewidth parameters) are then obtained from the effective one-body rigid rotor rates [37] which in turn are deduced from the detailed

state-to-state two-body rates by averaging over initial bath levels and summing over final bath levels. It should be noted that all the empirical rate law models entirely ignore the bath levels, using equations that would apply to excitation by a bath of structureless atoms. It can be shown that the effective one-body rates are independent of the initial bath molecule rotor level in the IOS approximation, [35] but this is no longer generally true if, for example, detailed balance is enforced or if a more accurate scattering treatment is used. In the current work the average over bath levels is done correctly, in contrast to rate law models where the dependence of effective one-body rates on initial bath rotational level must be absorbed into the temperature dependence of the fitted parameters.

In the next section we briefly review our recent, accurate CC and CS calculations [37] and compare these with linewidth data at room temperature and below. In the earlier work it was necessary to do a small amount of extrapolation of the CC-CS results to obtain all required thermal rates at 300 K for the higher rotational levels and Section III discusses the utility of such extrapolation schemes for predicting higher temperature CARS linewidths; in particular, we consider the utility of the ECS approximation using base rates obtained from the CC-CS calculations supplemented with new CS and IOS calculations at higher energies and compare with results of parameterized rate law models. Section IV presents a brief discussion of our findings.

II. LOW TEMPERATURE LINEWIDTHS

In our previous work [37] using the vdA [34] rigid rotor interaction we obtained state-to-state cross sections from CC calculations which were converged to generally better than 10% for total energies (relative kinetic plus internal rotor) to about 300 K; these are considered to be essentially exact results for the assumed interaction potential. We also obtained CS results to total energies of about 1000 K; these were shown to agree with CC to better than 15% at lower energies and their accuracy is expected to improve at the higher energies. These cross sections were averaged over a thermal distribution of collision energies at 300 K

and averaged and summed over bath rotational states to obtain effective one-body rates which were compared with the experimental values of Sitz and Farrow, [29] finding generally good agreement. Although these calculations were near the limit of current computational abilities, they were barely adequate to obtain all the rates needed for a room temperature thermal average, especially rates involving higher rotational levels, and we considered methods for extrapolating results to higher levels within the IOS/ECS framework. Two methods appeared to provide reasonable results. The first, designated CSX, simply took the CC-CS $R(0, 0 \rightarrow J_1, J_2)$ rates as the “fundamental rates” for IOS or ECS scaling; the second, designated LSQ, obtained these fundamental rates by a least-squares fit to the several thousand calculated CC-CS state-to-state rates.

In the present work we have calculated linewidth parameters, $W(J_1, J'_1)$, for the N_2 Q(J) Raman transitions by summing the two-body rates $R(J_1 J_2 \rightarrow J'_1 J'_2)$ obtained in the previous work over bath levels.

$$W(J_1, J'_1) = \sum_{J_2, J'_2} \rho(J_2) R(J_1 J_2 \rightarrow J'_1 J'_2), \quad J_1 \neq J'_1. \quad (1)$$

where $\rho(J_2)$ is the fraction of the bath molecules in rotational level J_2 . The linewidths, which are just the diagonal elements, $W(J_1, J_1)$, are then obtained from the sum rule,

$$\sum_{J'_1} W(J_1, J'_1) = 0. \quad (2)$$

Fig. 1 compares the experimental room temperature linewidths with values obtained using the available CC-CS rates. The CC-CS results are in excellent agreement with experimental values for lower rotational lines, to about $J = 9$, beyond which they begin to fall below experiment. As expected, the behavior at higher J reflects the lack of CC-CS rates required for a proper sum over bath levels and is corrected to some extent, as seen in Fig. 1, by the addition of CSX and LSQ extrapolated values which were computed as in our earlier work. However, it appears that predicted values from the LSQ scheme are too small and those from the CSX scheme too large; this is consistent with our previous conclusions. [37] Although the extrapolation schemes appeared to provide reasonable results for the state-to-

state rates, which are available only through $J = 14$, they do not appear to be adequate for the higher rotational levels probed by the linewidth data. We have therefore reconsidered the extrapolation schemes, especially the CSX scheme as it might be particularly useful for extending theoretical results to higher temperatures.

One somewhat surprising finding in the earlier work was that ECS corrections, i.e., a nonzero “scaling distance,” l_c , did not appear to improve agreement of the CSX results with the CC-CS state-to-state rates, although it did for the LSQ scheme in which l_c was fitted simultaneously with the base rates. There are, of course, many plausible measures of goodness of the fit, and our earlier work focused on relative error, especially the root mean square relative error; the LSQ fits, which are weighted least-squares fits, automatically minimize this quantity. For the CSX extrapolations the base rates are determined directly from CC-CS values and it was found that use of l_c values greater than zero steadily increased the root mean square relative error (and other measures of the absolute value of relative error). A closer examination indicates that rates predicted with $l_c = 0$ are almost always too large; in particular, predictions which are in error by more than 50% are invariably too large rather than too small. In general, using $l_c > 0$ lowers predictions for rates with larger inelasticity so that under predictions became comparable with over predictions. One measure of this is provided by the average signed error. Using $l_c = 0$ it is $1.5 \times 10^{-12} \text{ cm}^3\text{sec}^{-1}$ and using $l_c = 2.0$ it is $-3.3 \times 10^{-13} \text{ cm}^3\text{sec}^{-1}$. (These values can be compared with the average of all the rates in the data set, $7.9 \times 10^{-12} \text{ cm}^3\text{sec}^{-1}$.) This suggests that the use of $l_c = 2.0$ should give better predictions “on average,” in the sense of not being biased toward over or under prediction. Fig. 1 includes results obtained by augmenting CC-CS values with CSX using $l_c = 2.0$ which confirms this expectation; these predictions are seen to provide quite good agreement with all the room temperature experimental data.

Fig. 2 considers linewidths calculated entirely from CSX scaling predictions, i.e., ignoring the CC-CS values except insofar as they are used to obtain the “fundamental rates,” as a function of l_c ; experimental data and the CC-CS values are included for comparison. It is clear that $l_c = 0$ provides a significant over estimate when compared with the latter; the value

$l_c = 2.0$, on the other hand, provides rather good agreement with the CC-CS $Q(J)$ values over the low- J range where the latter are well determined. It turns out that a somewhat smaller value of $l_c = 1.75$ gives remarkably good agreement with the experimental values over the entire range; however, for our present purpose, which is to compare predictions of theoretical results from the vdA [34] potential with experimental values, we choose the value $l_c = 2.0$ as it provides the best agreement with the CC-CS values from this potential.

Herring and South [23] have recently measured linewidths at lower temperatures, presenting results for several $Q(J)$ lines at 113 K and for the $Q(10)$ line at several temperatures from 113 K to 298 K. We have performed Boltzmann averages of the CC-CS cross sections at the temperatures used by Herring and South. Results at 113 K are shown in Fig. 3 along with the experimental values. At this temperature nearly all the required state-to-state rates for the average over bath levels are available in the CC-CS data set; results which included CSX extrapolation (using $l_c = 2.0$) are included in the figure, but are seen to have little effect at this temperature. Unlike for room temperature, CC-CS values here over estimate the linewidths by 10–30%, strongly suggesting inaccuracies in the vdA interaction in regions sampled at lower energies.

Temperature dependence of the $Q(10)$ line is shown in Fig. 4. Predictions of the CC-CS calculation, which are in reasonable agreement with experiment at room temperature, are seen to become increasingly too large as the temperature is decreased. Again, this presumably reflects errors in the interaction potential in regions which become more important at lower collision energies. In addition to the pure CC-CS results, values supplemented with CSX ($l_c = 2.0$) extrapolated rates for higher rotational levels are also shown. The increasing need at higher temperature to use such extrapolated values is clearly evident.

III. HIGH TEMPERATURE LINEWIDTHS

The apparent accuracy of the CSX extrapolation scheme at room temperature and below suggested a possible method for extending calculations to higher temperatures. CS

calculations for the “fundamental,” $\sigma(0, 0 \rightarrow J_1, J_2)$, cross sections which are needed for the CSX extrapolation are significantly cheaper than calculations for the entire matrix of cross sections since only the block with zero projection quantum number is required. Also, for a system such as this with homonuclear symmetry, calculations are required only for (even J -even J) rotor functions. Accordingly, we have done new CS calculations for energies from 680 to 840 cm^{-1} using a basis of the lowest 100 levels (distinguishable molecule counting), and from 900 to 1050 cm^{-1} using a basis of the lowest 123 levels; the largest calculations involved 1411 coupled channels.

Unfortunately, even this larger range of collision energies was only marginally adequate for Boltzmann averages at 500 and 730 K, especially for transitions with large ΔJ , where cross sections are increasing rapidly near the upper end of the energy range, and it was certainly not adequate for predicting values at 1000 and 1500 K for which data are also available. We therefore reconsidered the utility of the infinite order sudden (IOS) approximation [35] for obtaining values for the fundamental cross sections. In many cases these higher energies contribute only a modest fraction of the Boltzmann average, so it is necessary only to have a reasonable estimate of the high energy behavior. In principle, the IOS approximation becomes more accurate at high enough energies.

Because the IOS approximation ignores the rotor energies compared with the collision kinetic energy there is some ambiguity concerning the energy which should be associated with a calculated IOS cross section. It is also desirable to enforce the requirement of detailed balance between forward and reverse transitions which is lost in the IOS approximation. Chapman and Green [45] considered several possibilities, finding that some appeared to give better agreement with more accurate values. In particular, equating the IOS energy to the final energy for either upward or downward transitions or to the initial energy averaged over upward and downward transitions appeared to be most reasonable. These can be described by

$$\sigma_{FU}^{IOS}(0, 0 \rightarrow J_1, J_2; E + \Delta E) = Q_{J_1, J_2}(E) \quad (3)$$

$$\sigma_{FD}^{IOS}(0, 0 \rightarrow J_1, J_2; E) = \frac{E - \Delta E}{E} Q_{J_1, J_2}(E) \quad (4)$$

$$\sigma_{IA}^{IOS}(0, 0 \rightarrow J_1, J_2; E + \Delta E/2) = \frac{E}{E + \Delta E/2} Q_{J_1, J_2}(E) \quad (5)$$

Here $Q_{J_1, J_2}(E)$ is the generalized IOS cross section [35,45] calculated at a collision energy E and ΔE is the excitation energy. In some cases the collision energy associated with the cross section is shifted from that used in the IOS calculations and in some cases the IOS cross section is also scaled by an energy factor. In the present work all three of these choices were tried for IOS collision energies from 400–2500 cm⁻¹ and compared with the available CS results.

For transitions with small inelasticity (i.e., small J_1, J_2) and, in general, at the highest energies, all three prescriptions give similar results, as expected. However, for most transitions, σ_{FU}^{IOS} appeared consistently to give the most reasonable behavior compared with the high energy CS results, and therefore these were used for the Boltzmann averages. At the highest temperatures inclusion of base rates through $J_1, J_2 = 20$ was required; in some cases no CS values were available and rates were obtained exclusively from the σ_{FU}^{IOS} values. In this way CSX base rates were obtained at 300, 500, 730, 1000, and 1500 K. These were used with ECS scaling to predict CARS linewidths which are compared with experimental values in Figs. 5–9. If this method is to have any predictive ability the value for the ECS scaling length, l_c , must be obtainable from the lower temperature results. We accordingly used the value, $l_c = 2.0$, which gave the best agreement with CC-CS rates at 300 K, and these predictions are shown by the solid lines; values obtained with somewhat smaller values of l_c are shown as dashed lines.

A careful comparison of Figs. 5 and 2 indicates an apparent discrepancy: in the latter a value of $l_c = 1.75$ gives the best agreement with experiment, but in the former it is $l_c = 2.0$. In fact, the 300 K predictions for a given l_c in Fig. 5 are uniformly larger than those in Fig. 2 — by about 5% at for low J and about 15% at higher J . This results from changes in the 300 K base rates when the higher energy CS and IOS values are included. Although

the differences are only a percent or two for base rates with $J_1, J_2 \leq 10$, the changes in some of the higher base rates are much larger, and these become important for the higher Q(J) lines. It is noteworthy that the value of $l_c = 2.0$, which was selected by comparing CSX predictions with the earlier CC-CS rate matrix provides excellent agreement with all the experimental CARS linewidths at 300 K.

Predictions for the higher temperature data are, in general, in quite reasonable agreement with the experimental data, although the disparities show certain regularities which are probably significant. The most obvious is that a smaller l_c value appears to be more appropriate for higher temperatures and for higher Q(J) lines. This is physically plausible as these cases are expected to be more influenced by closer collisions; a similar effect was noted in earlier results based only on IOS calculations. [35] In that work the value of $l_c = 2.0$ was found to give good agreement with room temperature data, the same value as found in the present study, but a value of $l_c = 1.0$ was found to be more appropriate for 1500 K data. Unfortunately, the dependence of the critical impact parameter on temperature and on spectral level diminishes the utility of ECS scaling as a predictive method. Some discrepancies also occur for lines with small to moderate J where theory tends to underestimate experimental values. However, the trend here with temperature and with rotational level is less clear and it is difficult to pin the discrepancies on problems with the CSX extrapolation procedure, errors in the potential, or inaccuracies in the experimental values.

The CSX method is closely related to the most successful of the parameterized rate law models used to analyze CARS data, the ECS-EP model. [13,46] This model uses the ECS approximation as does the CSX scaling, but the fundamental rates are calculated from a four parameter hybrid exponential-polynomial (EP) rate law with parameters fitted to the experimental data, the scaling length, l_c being a fifth fitting parameter. By contrast, fundamental rates in the CSX method are obtained from first principles calculations on an interaction potential which has been determined separately, and l_c is determined from fitting to the complete ab initio rate matrix. A second difference is that the CSX model uses the ECS approximation for two-body rates, [35,37] performing a proper average and sum

over the bath levels, whereas the ECS-EP model treats the bath molecules as if they were structureless atoms. Millot [13] has obtained ECS-EP parameters for $\text{N}_2\text{-N}_2$ by fitting to the data presented in Figs. 5–9; predictions from that fit are included for comparison with experiment and with the CSX values. Not surprisingly the ECS-EP predictions are rather similar to the CSX results.

In order to quantify the accuracy of these two methods, root-mean-square deviations between predictions and experimental values are presented in Table I for each temperature and for the combined data sets. Also presented are statistics for the deviation between experimental and predicted value divided by the reported experimental uncertainty for each line; thus, values less than one are within the experimental error. It is not surprising that the ECS-EP values agree somewhat better with the data as the parameters in this model were optimized to reproduce the data, whereas the CSX values, which were obtained entirely from first principles, reflect inaccuracies in the interaction potential as well as approximations to the collision dynamics. Considering that ECS-EP is the most successful of a long series of increasingly more sophisticated attempts to fit these linewidth data, [46] the CSX values are seen to be remarkably good. Note that the ECS-EP values, like the CSX values are too small for high temperatures and high rotor levels, a problem we attributed to use of a fixed value for l_c .

It is interesting to consider how well the ECS-EP model is able to predict the low temperature data which were obtained more recently and which were not included in fitting the model parameters. The 113 K data are shown in Fig. 10 along with ECS-EP values and CSX values using $l_c = 2.0$. It is seen that the ECS-EP model does not do particularly well when extended to temperatures outside the range for which the parameters were fitted; this point was noted by Herring and South [23] in connection with their low temperature measurements. The good agreement of CSX results with experiment here, however, must also be considered somewhat fortuitous since they are significantly lower than the CC-CS values (see Fig. 3) which accurately reflect collision dynamics on the vdA potential at this temperature. Note that better agreement of CSX values with the 113 K CC-CS values could

be obtained by using a smaller value of l_c , but this is inconsistent with the finding that smaller values of l_c are more appropriate at *higher* temperatures. Rather, the CSX method, which relies on ECS corrections to the IOS approximation, must eventually break down at low enough temperatures since the IOS approximation itself becomes less good and the ECS *estimates* for these larger corrections then become unreliable.

IV. DISCUSSION

Accurate CC-CS state-to-state cross sections calculated with the vdA [34] interaction provide good agreement with experimental room temperature CARS linewidths up to $J = 9$. Discrepancies for Q(J) lines with $J > 9$ resulted from lack of theoretical cross sections among higher rotational levels, but, by estimating these using the ECS scaling relations with fundamental rates obtained from the CC-CS results, good agreement was obtained through $J = 18$, the highest line measured. For temperatures below room temperature CC-CS predictions became increasingly larger than experimental values, with errors reaching about 25% at 113 K. Since these calculations used accurate dynamics, the discrepancies presumably reflect inaccuracies in the potential in regions that are more important for low energy collisions; this is consistent with conclusions of Heck and Dickinson. [36]

For temperatures above 300 K we used CSX scaling, including higher energy CS and IOS cross sections to obtain the fundamental rates and choosing the scaling distance by fitting to the 300 K matrix of CC-CS rates. This provides rather good agreement with CARS linewidth data through 1500 K. Agreement is nearly as good as that obtained from the best rate law model, the ECS-EP model, whose five parameters were obtained by fitting to the CARS linewidth data. [13] Comparison of both the CSX scaling results and the ECS-EP rate law model with experimental data appear to suggest that the ECS scaling length, l_c should not be fixed, but should decrease for higher temperatures and for higher rotational levels. However, the scaling methods used at higher temperatures, although based on well defined approximations, are of unknown accuracy, and the remaining discrepancies with

experiment might also come from inaccuracies in the vdA potential in regions sampled by higher energy collisions. There is some evidence from comparisons with solid state data that the vdA interaction is too repulsive at small intermolecular separations. [34] A new interaction potential for this system has been obtained recently by Partridge and Stallcop using more sophisticated quantum chemistry methods, [47] and it appears to be less repulsive at short distances; it also differs somewhat from the vdA interaction in the van der Waals region. It will be interesting to test this potential by comparing with the extensive linewidth data.

Although we believe that the CSX extrapolation scheme used here does have utility, it would be preferable to calculate directly the rates among higher levels and for higher collision energies using methods of known accuracy; this is especially important if comparisons with high temperature data are used to assess accuracy of the interaction. Increases in computational power will make it possible to extend coupled channel methods somewhat, but calculations for the highest temperatures of interest here are not likely to be possible in the near future. A method which deserves closer scrutiny is quasiclassical trajectories (QCT). QCT is known to provide reliable results for rotational excitation of linear molecules by collisions with atoms, [48] but such calculations also become rather expensive for collisions of two linear molecules owing to the number of trajectories required to obtain good statistics when there are many possible initial states and many final state bins. However, for pressure broadening cross sections one can include the initial bath molecule distribution in the Monte Carlo averaging, simply summing over final bath molecule states. If effective one-body rates are not required, but only linewidth cross sections, one can also sum over all final levels of the spectral molecule, making QCT calculations particularly attractive for this problem.

Finally, the role of identical molecule symmetry in linewidth calculations is a factor not considered in this or previous studies. Although exchange effect is believed to be small, no study has yet been made to determine its magnitude or its temperature and J dependence. Only future studies, with exchange symmetry properly accounted for, can determine whether exchange is the source of some of the discrepancies with experiment observed here.

ACKNOWLEDGMENTS

SG is supported by NASA Headquarters, Office of Space Science and Applications, Astrophysics Division. The large scale computations in this study were made possible through a grant of Cray C90 time from the Numerical Aerodynamic Simulation Facility.

REFERENCES

- [1] K. S. Jammu, G. E. St. John, and H. L. Welsh, *Can. J. Phys.* **44**, 797 (1966).
- [2] G. J. Rosasco, W. Lempert, W. S. Hurst, and A. Fein, *Chem. Phys. Lett.* **97**, 435 (1983).
- [3] D. A. Greenhalgh, F. M. Porter, and S. A. Barton, *J. Quant. Spectrosc. Radiat. Transfer* **34**, 95 (1985).
- [4] J. P. Sala, J. Bonamy, D. Robert, B. Lavorel, G. Millot, and H. Berger, *Chem. Phys.* **106**, 427 (1986).
- [5] L. A. Rahn and R. E. Palmer, *J. Opt. Soc. Am. B* **3**, 1164 (1986).
- [6] B. Lavorel, G. Millot, R. Saint-Loup, C. Wenger, H. Berger, J. P. Sala, J. Bonamy, and D. Robert, *J. Phys. (Paris)* **47**, 417 (1986).
- [7] G. C. Herring, M. J. Dyer, and W. K. Bischel, *Phys. Rev. A* **34**, 1944 (1986).
- [8] M. L. Koszykowski, L. A. Rahn, R. E. Palmer, and M. E. Coltrin, *J. Phys. Chem.* **91**, 41 (1987).
- [9] B. Lavorel, R. Chaux, R. Saint-Loup, and H. Berger, *Opt. Commun.* **62**, 25 (1987).
- [10] B. Lavorel, G. Millot, J. Bonamy, and D. Robert, *Chem. Phys.* **115**, 69 (1987).
- [11] L. A. Rahn, R. E. Palmer, M. L. Koszykowski, and D. A. Greenhalgh, *Chem. Phys. Lett.* **133**, 513 (1987).
- [12] L. Bonamy, J. Bonamy, D. Robert, B. Lavorel, R. Saint-Loup, R. Chaux, J. Santos, and H. Berger, *J. Chem. Phys.* **89**, 5568 (1988).
- [13] G. Millot, *J. Chem. Phys.* **93**, 8001 (1990).
- [14] M. L. Gonze, R. Saint-Loup, J. Santos, B. Lavorel, R. Chaux, G. Millot, H. Berger, L. Bonamy, J. Bonamy, and D. Robert, *Chem. Phys.* **148**, 417 (1990).

- [15] L. Bonamy, J. M. Thuet, J. Bonamy, and D. Robert, J. Chem. Phys. **95**, 3361 (1991).
- [16] S. Temkin, J. M. Thuet, L. Bonamy, J. Bonamy, and D. Robert, Chem. Phys. **158**, 89 (1991).
- [17] J. P. Looney and G. J. Rosasco, J. Chem. Phys. **95**, 2379 (1991).
- [18] B. Oksengorn, D. Fabre, B. Lavorel, R. Saint-Loup, and H. Berger, J. Chem. Phys. **94**, 1774 (1991).
- [19] B. Lavorel, B. Oksengorn, D. Fabre, R. Saint-Loup, and H. Berger, Molec. Phys. **75**, 397 (1992).
- [20] L. Martinsson, P.-E. Bengtsson, M. Aldén, S. Kröll, and J. Bonamy, J. Chem. Phys. **99**, 2466 (1993).
- [21] Y. I. Bulgakov, A. V. Storozhev, and M. L. Strekalov, Chem. Phys. **177**, 145 (1993).
- [22] T. Dreier, G. Schiff, and A. A. Suvernev, J. Chem. Phys. **100**, 6275 (1994).
- [23] G. C. Herring and B. W. South, J. Quant. Spectrosc. Radiat. Transfer **52**, 835 (1994).
- [24] D. A. Greenhalgh, in *Advances in Non-Linear Spectroscopy*, edited by R. J. H. Clark and R. E. Hester (Wiley, New York, 1988), p. 193.
- [25] R. J. Exton and M. E. Hillard, Appl. Opt. **25**, 14 (1986); R. R. Antcliff, M. W. Smith, O. Jarret, Jr., A. Cutler, G. B. Northam, and D. J. Taylar, AAIA-91-0457, “A hardened CARS system utilized for temperature measurements in a supersonic combustor,” presented at the 29th Aerospace Sciences Meeting, 7-10 January 1991, Reno, NV.
- [26] F. Thibault, J. Boissoles, R. Le Doucen, R. Farrenq, M. Morillon-Chapey, and C. Boulet, J. Chem. Phys. **97**, 4623 (1992).
- [27] P. M. Sinclair, J. W. Forsman, J. R. Drummond, and A. D. May, Phys. Rev. A **48**, 3030 (1993).

- [28] C. Park, *Nonequilibrium Hypersonic Aerothermodynamics*, (Wiley, New York, 1990).
- [29] G. O. Sitz and R. L. Farrow, J. Chem. Phys. **93**, 7883 (1990).
- [30] A. E. Belikov, R. G. Sharafutdinov, M. L. Strekalov, Chem. Phys. Lett. **231**, 444 (1994).
- [31] G. O. Sitz and R. L. Farrow, J. Chem. Phys. **101**, 4682 (1994); *erratum*, J. Chem. Phys. **103**, 489 (1995).
- [32] P. J. Agg and D. C. Clary, Molec. Phys. **73**, 317 (1991).
- [33] G. D. Billing and L. Wang, J. Phys. Chem. **96**, 2572 (1992).
- [34] A. van der Avoird, P. E. S. Wormer, and A. P. J. Jansen, J. Chem. Phys. **84**, 1629 (1985).
- [35] S. Green, J. Chem. Phys. **98**, 257 (1993); *erratum*, J. Chem. Phys. **99**, 4875 (1993).
- [36] E. L. Heck and A. S. Dickinson, Molec. Phys. **81**, 1325 (1994).
- [37] W. M. Huo and S. Green, J. Chem. Phys. submitted.
- [38] S. Green, in *Status and Future Developments in Transport Properties*, edited by W. A. Wakeham, *et al.* (Kluwer Academic, Amsterdam, 1992), pp. 257-283.
- [39] U. Fano, Phys. Rev. **131**, 259 (1963).
- [40] A. Ben-Reuven, Phys. Rev. **145**, 7 (1966).
- [41] A. Ben-Reuven, Phys. Rev. A **4**, 2115 (1971).
- [42] R. A. Pasmanter and A. Ben-Reuven, J. Quant. Spectrosc. Radiat. Transfer **13**, 57 (1973).
- [43] W.-K. Liu, J. Chem. Phys. **72**, 4869 (1980).
- [44] L. Monchick, J. Chem. Phys. **101**, 5666 (1994).
- [45] S. Chapman and S. Green, Chem. Phys. Lett. **112**, 436 (1984).

- [46] J. I. Steinfeld, P. Ruttenberg, G. Millot, G. Fanjoux, and B. Lavorel, J. Phys. Chem. **95**, 9638 (1991).
- [47] H. Partridge and J. R. Stallcop, in preparation.
- [48] S. Chapman and S. Green J. Chem. Phys. **67**, 2317 (1977).

TABLES

TABLE I. Root mean square errors from CSX/ $l_c=2.0$ and ECS-EP predictions of CARS linewidths. Relative error is the difference between theory and experiment divided by the reported experimental uncertainty.

| T, Kelvin | N ^a | rms error, $10^{-3}\text{cm}^{-1}/\text{atm}$ | | rms relative error | |
|-----------|----------------|---|--------|--------------------|--------|
| | | CSX | ECS-EP | CSX | ECS-EP |
| 300 | 19 | 3.0 | 2.3 | 0.50 | 0.30 |
| 500 | 27 | 3.3 | 2.4 | 1.36 | 1.07 |
| 730 | 25 | 3.0 | 2.1 | 1.79 | 1.15 |
| 1000 | 27 | 2.4 | 2.2 | 2.06 | 1.82 |
| 1500 | 25 | 3.2 | 2.9 | 2.82 | 2.57 |
| all data | 123 | 3.0 | 2.4 | 1.91 | 1.61 |

^aNumber of data points.

FIGURES

FIG. 1. Comparison of experimental room temperature CARS linewidths [5] with CC-CS predictions and CC-CS predictions augmented with various extrapolation schemes for the missing rates among higher levels.

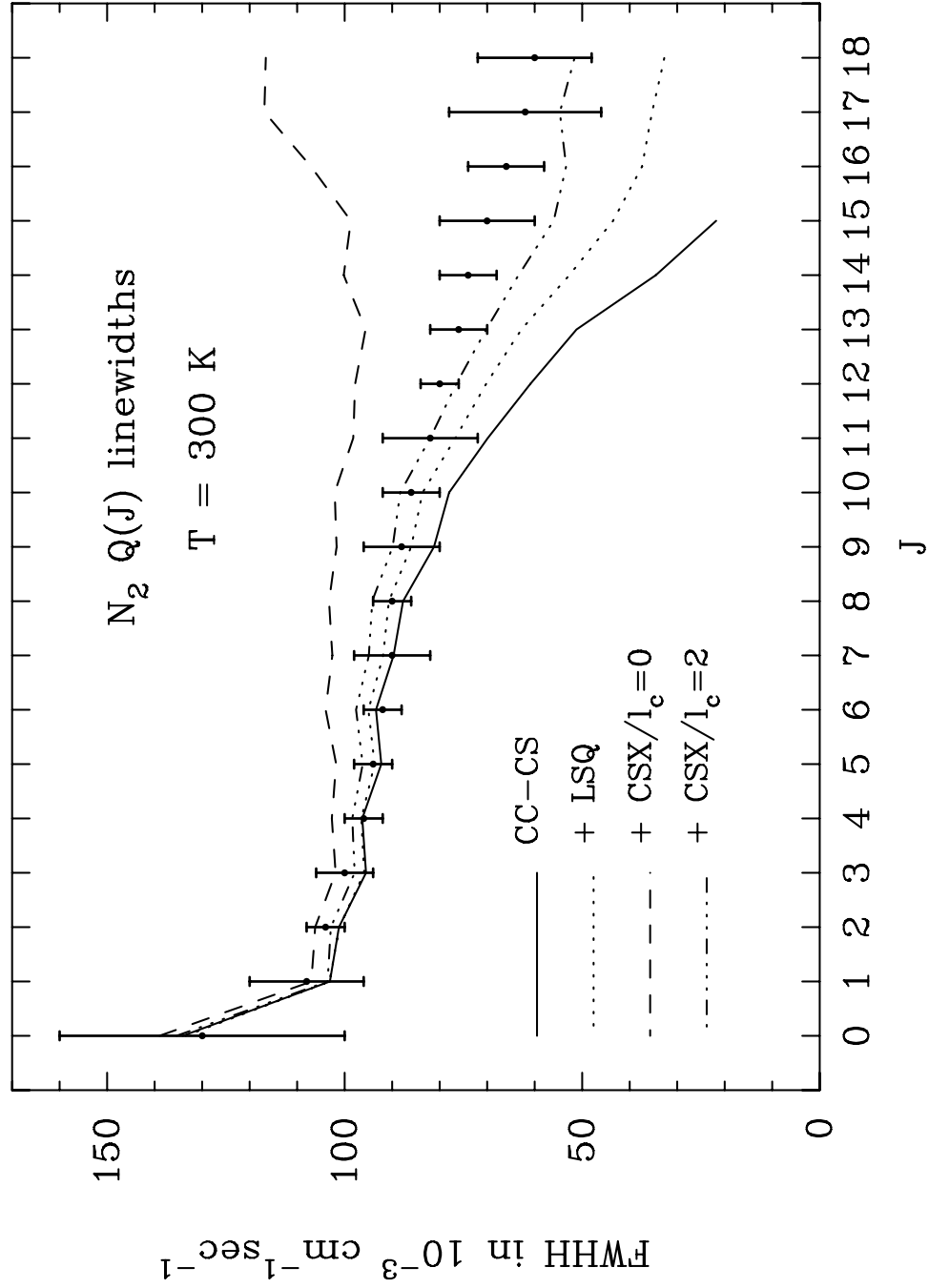


FIG. 2. Room temperature linewidths predicted by the CSX extrapolation scheme using varying l_c are compared with CC-CS values and with experimental [5] data.

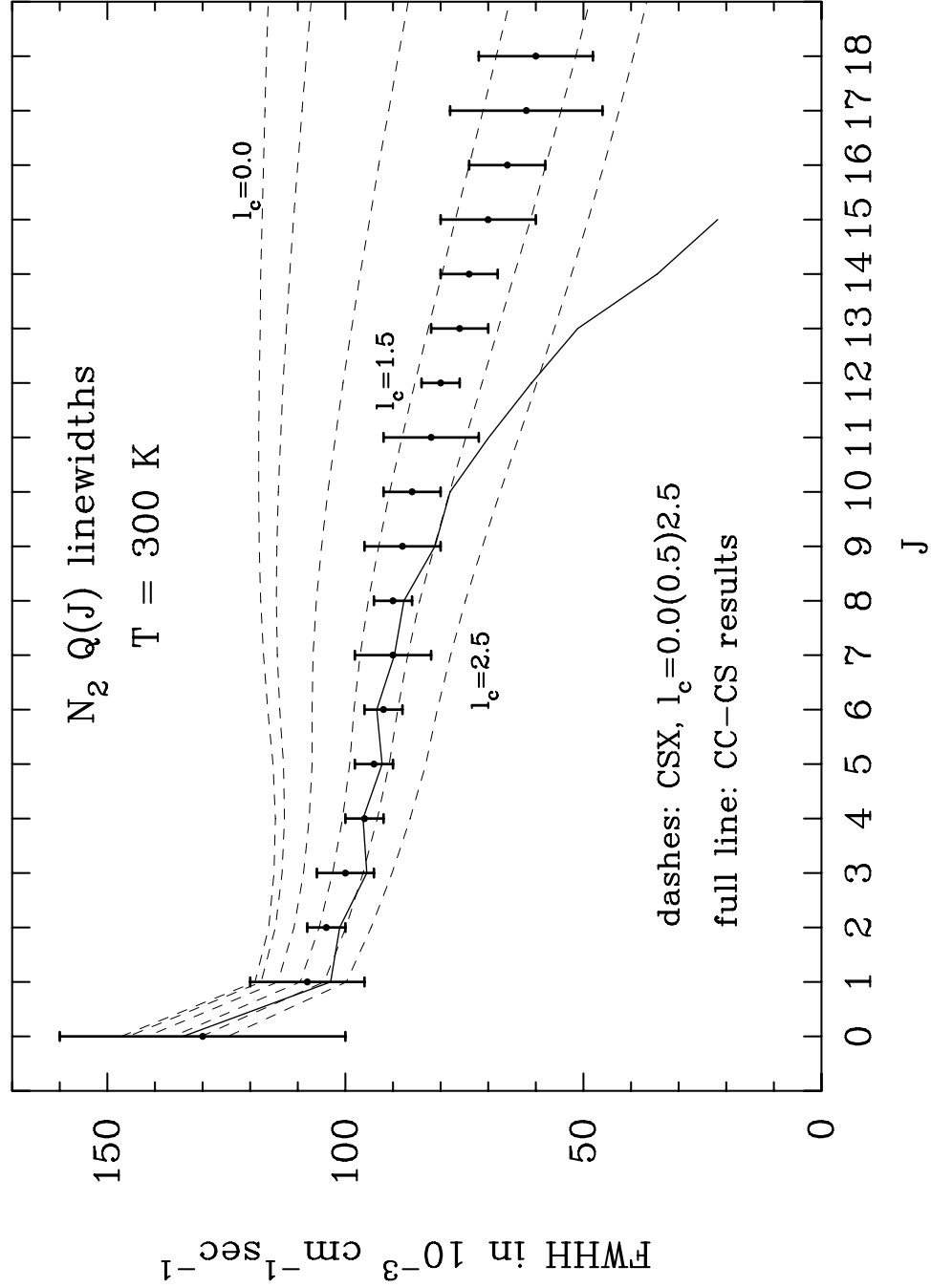


FIG. 3. Comparison of experimental [23] 113 K CARS linewidths with CC-CS predictions and CC-CS predictions augmented with CSX extrapolation.

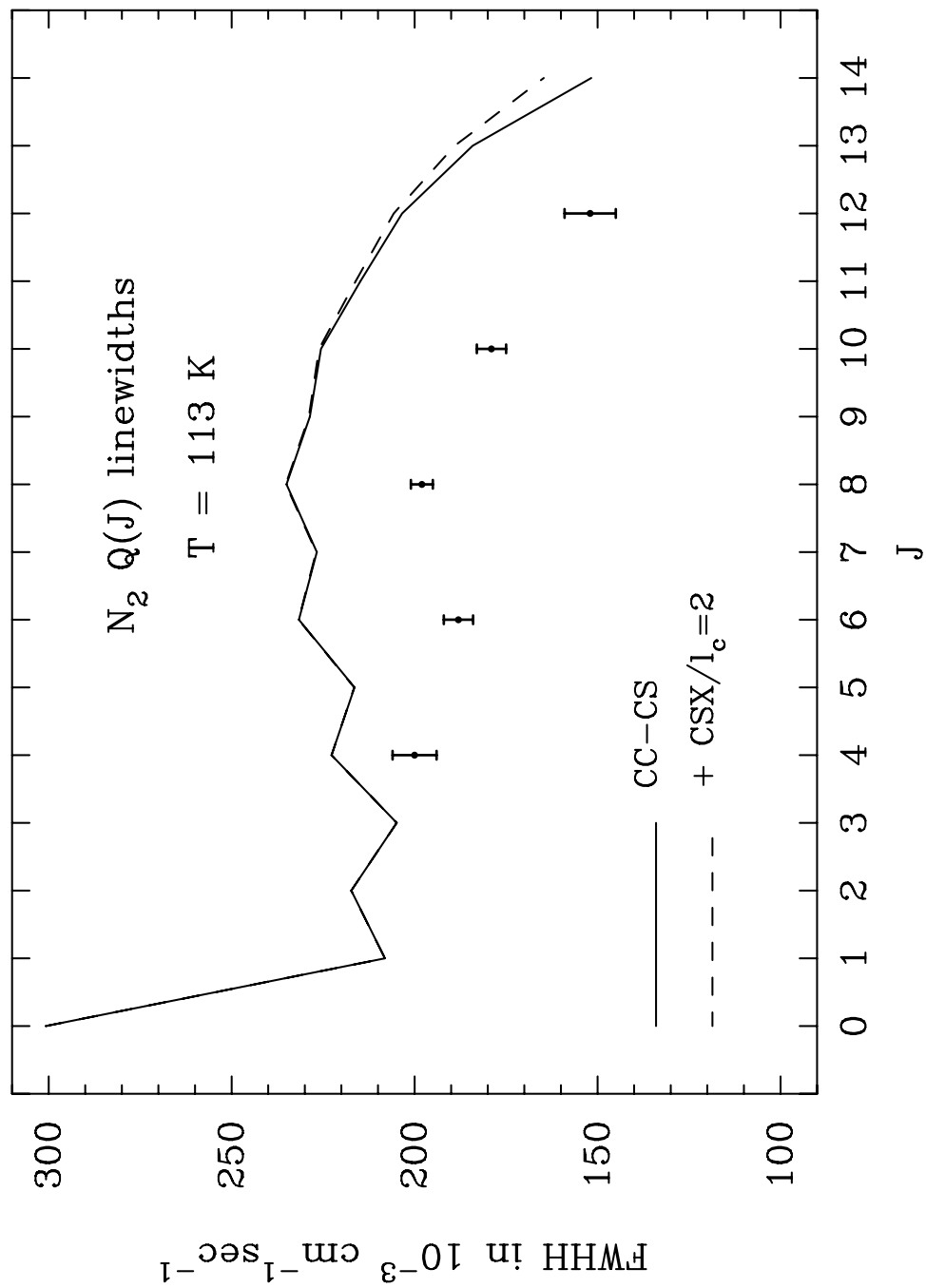


FIG. 4. Experimental [23] $Q(10)$ linewidths as a function of temperature are compared with predictions from CC-CS calculations and from CC-CS augmented with CSX extrapolation.

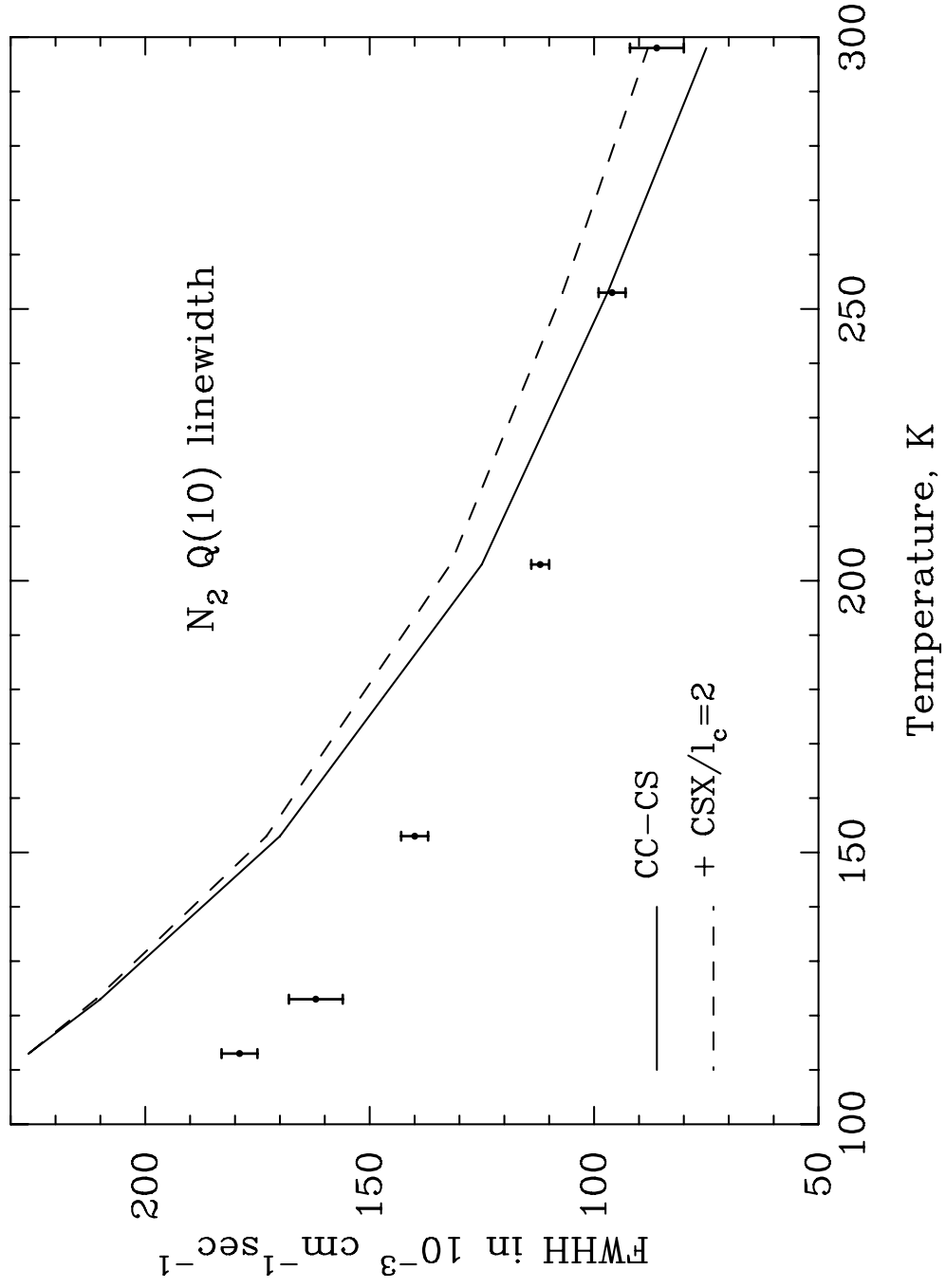


FIG. 5. CARS $Q(J)$ linewidths at 300 K predicted from CSX extrapolation using base rates that included higher energy CS and IOS values are compared with experimental [5] values. Predictions of the ECS-EP rate law model [13] are also shown.

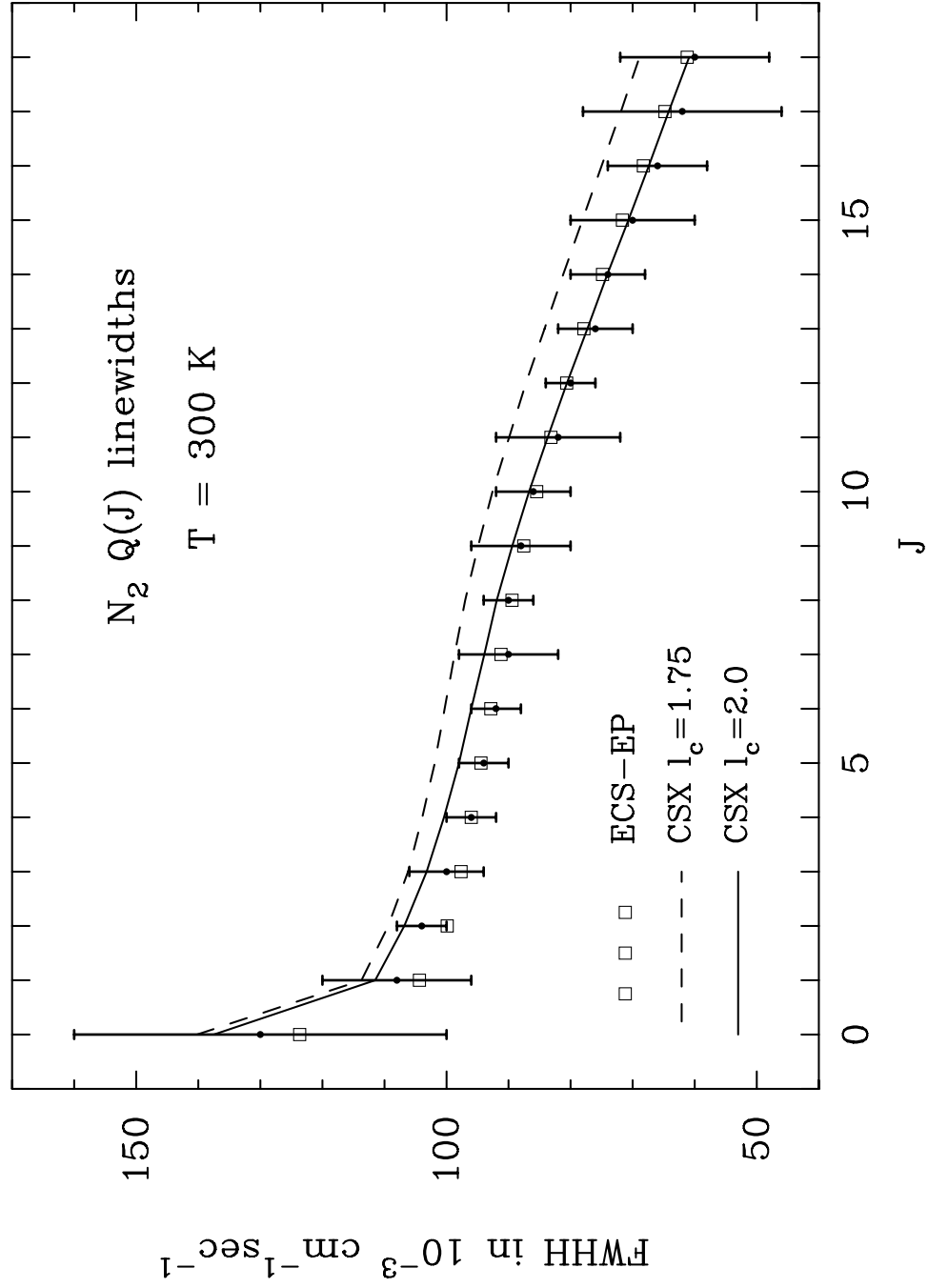


FIG. 6. CARS $Q(J)$ linewidths at 500 K predicted from CSX extrapolation using base rates that included higher energy CS and IOS values are compared with experimental [5] values. Predictions of the ECS-EP rate law model [13] are also shown.

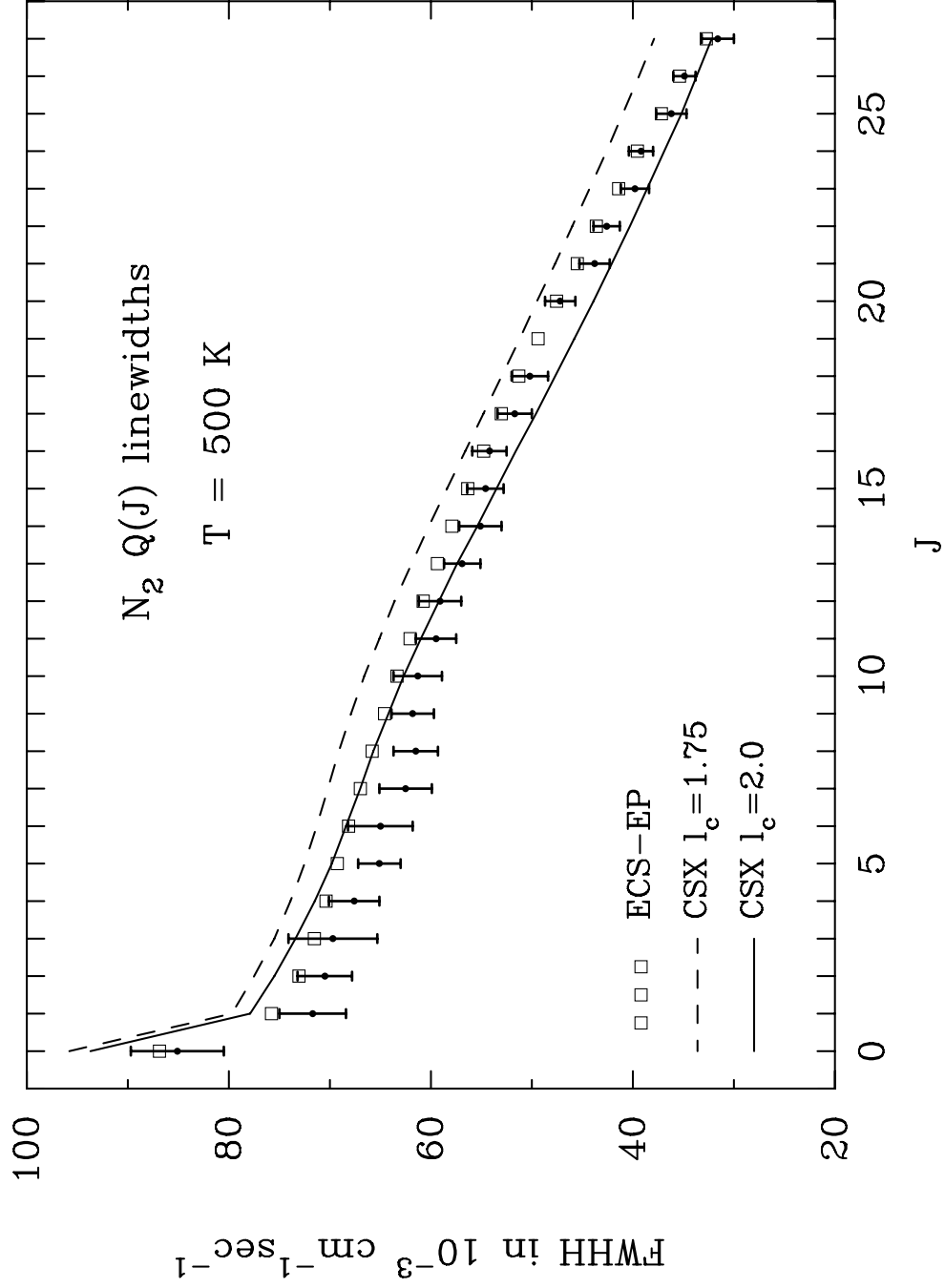


FIG. 7. CARS $Q(J)$ linewidths at 730 K predicted from CSX extrapolation using base rates that included higher energy CS and IOS values are compared with experimental [5] values. Predictions of the ECS-EP rate law model [13] are also shown.

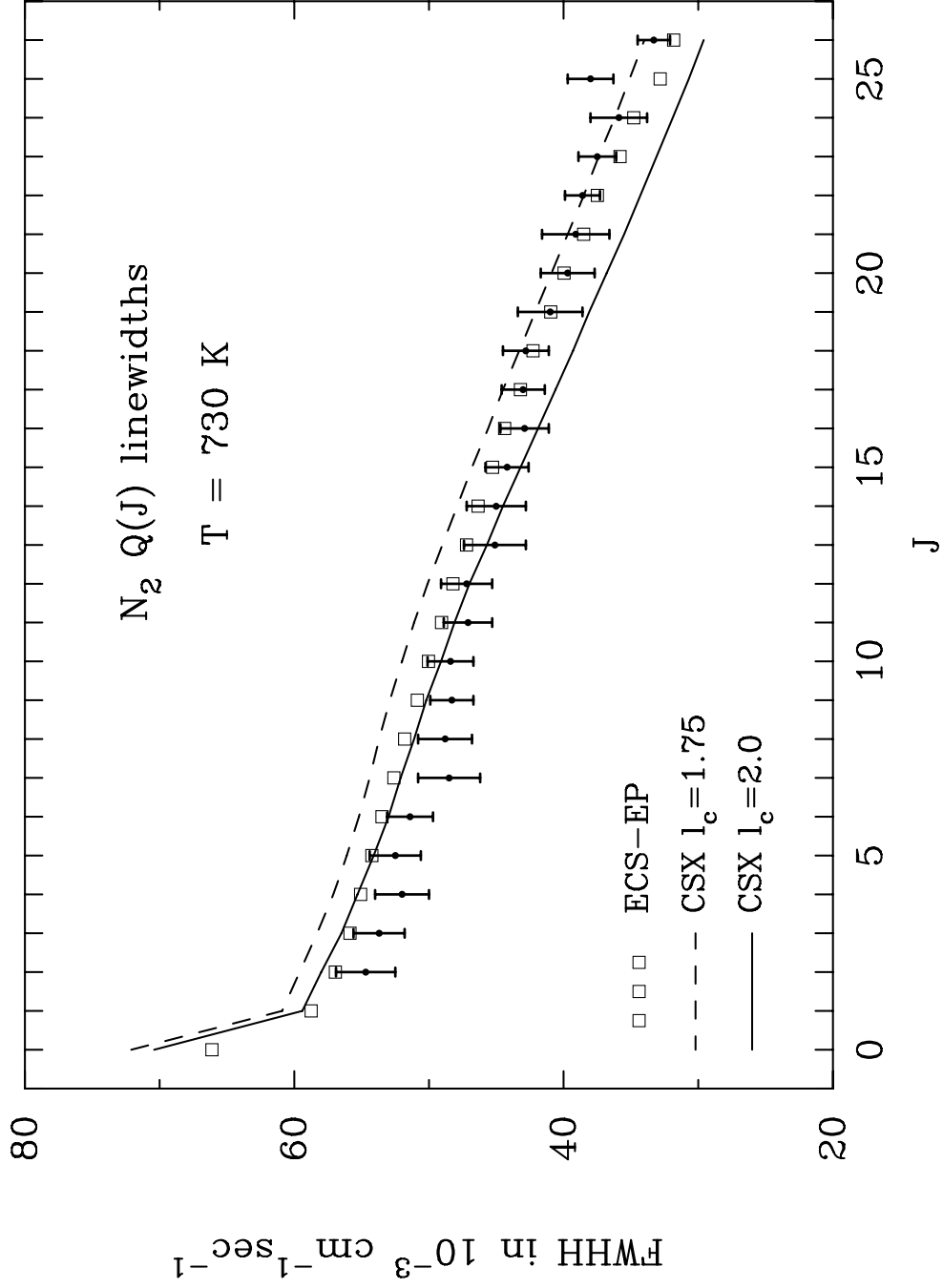


FIG. 8. CARS $Q(J)$ linewidths at 1000 K predicted from CSX extrapolation using base rates that included higher energy CS and IOS values are compared with experimental [5] values. Predictions of the ECS-EP rate law model [13] are also shown.

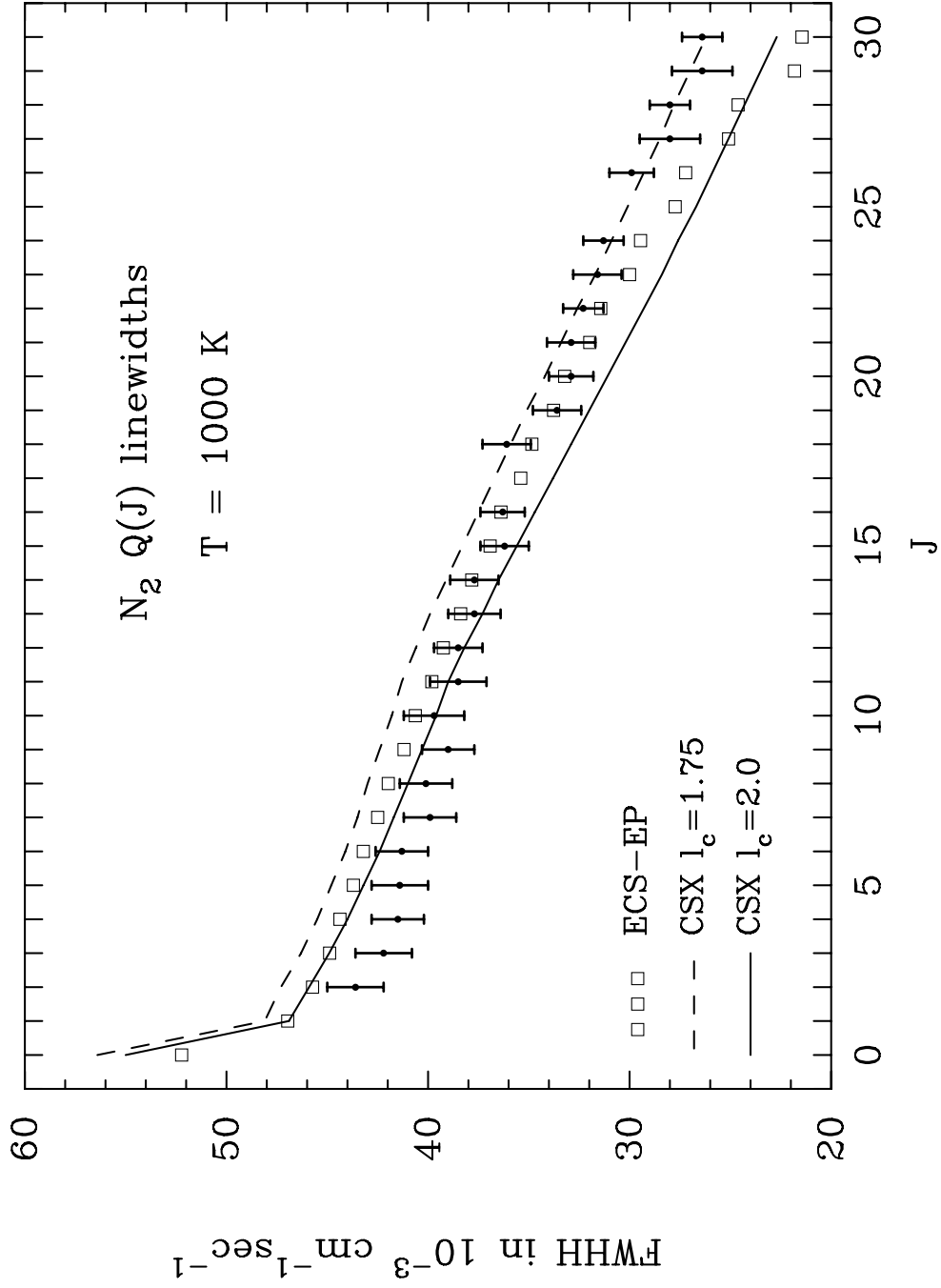


FIG. 9. CARS $Q(J)$ linewidths at 1500 K predicted from CSX extrapolation using base rates that included higher energy CS and IOS values are compared with experimental [5] values. Predictions of the ECS-EP rate law model [13] are also shown.

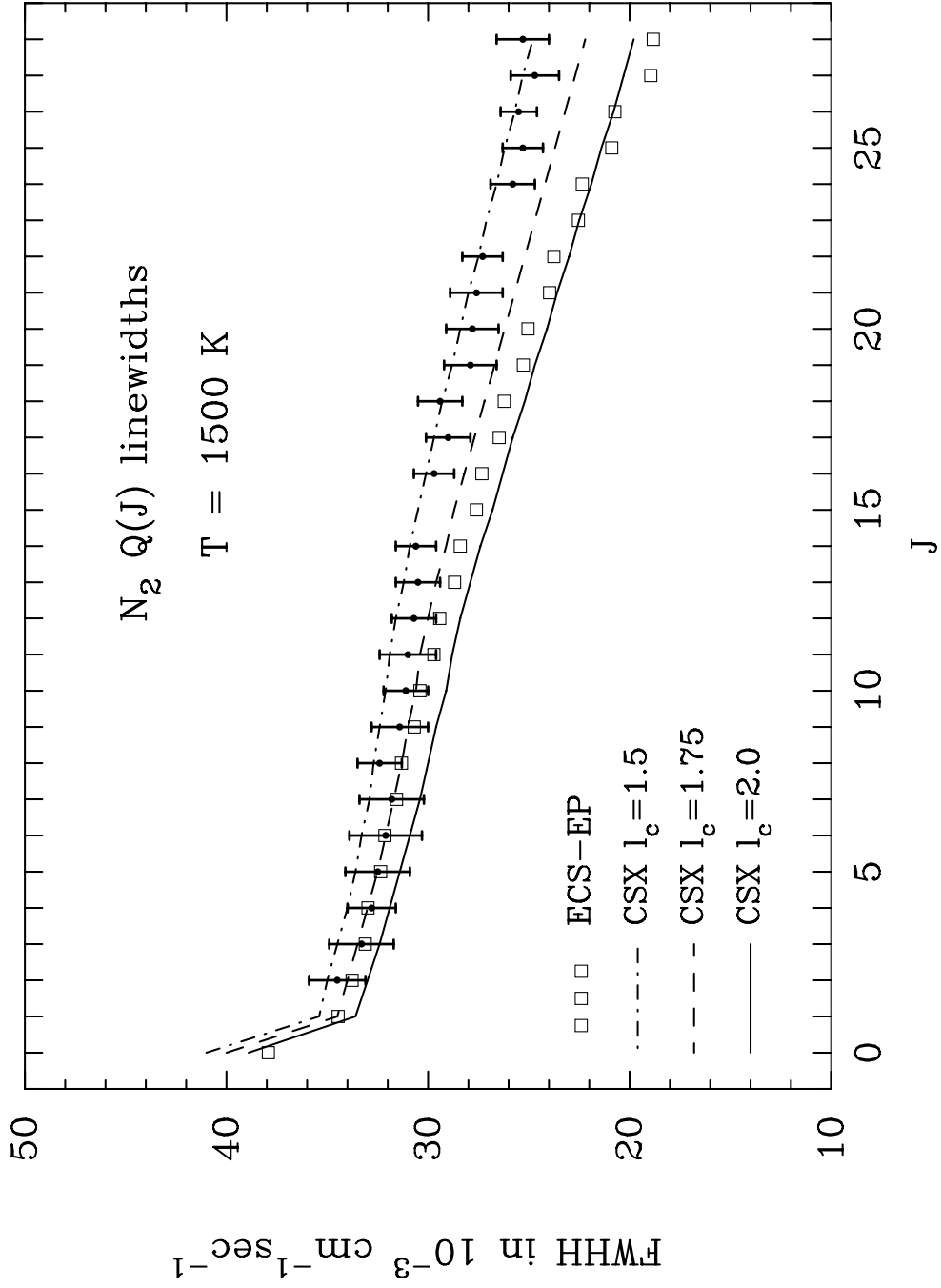


FIG. 10. Experimental CARS $Q(J)$ linewidths at 113 K [23] are compared with predictions of the CSX extrapolation using a value of $l_c = 2.0$ and with predictions of the ECS-EP rate law model. [13]

